Subcortical substrates of TMS induced modulation of the cortico-cortical connectivity

Sergiu Groppa [a,*,1], Muthuraman Muthuraman [a,1], Birte Otto [a], Günther Deuschl [a], Hartwig R. Siebner [a,b,1], Jan Raethjen [a,1]

[a] *Department of Neurology, Christian-Albrechts University, Schittenhelmstr 10, Kiel 24105, Germany*
[b] *Danish Research Centre for Magnetic Resonance, MR-Department, Copenhagen University Hospital Hvidovre, Hvidovre, Denmark*

Introduction

Transcranial magnetic stimulation (TMS) has been used for more than 20 years to study connectivity and plasticity in human cortex. The magnetic pulse induces a time varying electrical current in the underling cerebral tissue. Suprathreshold pulses elicit action potentials in the stimulated cells and generate volleys that proceed along certain stimulated pathways [6]. The stimulation of the primary motor cortex (M1) evolves in discharges of the cortico-spinal motoneurons that can be recorded as muscle evoked potentials (MEP). These are a reliable marker of cortical excitability [10,13]. Moreover a single TMS pulse does not only change the neural activity in the stimulated area but modulates also the excitability of interconnected distant sites [34]. Furthermore a TMS pulse can induce a synchronisation of distant cortical areas in this way modulating the information processing and changing the functional connectivity patterns in specialised interconnected cortical modules [19,29]. Combined TMS-EEG approaches have been introduced to study and quantify cortical connectivity patterns [40,43]. A recent study demonstrated that TMS can induce oscillations at different frequencies, depending on the cortical stimulation site [32]. It has been postulated that these TMS induced oscillations reflect physiological activity that is transiently enhanced by the TMS pulse. Thus combined TMS-EEG recordings are a procedure to study the physiological oscillatory interactions on an enlarged scale [40]. TMS induced synchronization has been

The authors have reported no conflicts of interest.

SG was funded by an intern grant of University of Kiel. JR and MM were funded by a DFG Grant of SFB 855 "Magnetoelectric Composites - Future Biomagnetic Interfaces". HRS received additional support by the Bundesministerium für Bildung und Forschung (01GO0511 'NeuroImageNord') and a Grant of Excellence from The Lundbeck Foundation Mapping, Modulation & Modelling the Control of Actions (ContAct) (R59 A5399).

* Corresponding author. Tel.: +49 431 597 8823; fax: +49 431 597 8502.
E-mail address: s.groppa@neurologie.uni-kiel.de (S. Groppa).

[1] These authors contributed equally to the manuscript.

observed in both alpha and beta bands [9,29]. After a supra-threshold TMS pulse over M1 Fuggetta et al. showed that alpha band oscillations were a dominant rhythm evolving and there was an increased cortico-cortical coupling in this frequency domain [9]. In line with previous studies the authors postulate a common thalamic pacemaker that modulates the ongoing oscillatory activity and links the information flow between different cortical areas possibly through thalamocortical loops [5,9,37]. Although there is ample evidence from animal experiments about the structure and function of these loops, direct evidence about these thalamocortical pathways in humans is sparse [17,37]. Whether the thalamic pacemakers, the cortico-cortical projections or the thalamocortical pathways contribute to the intra- or interhemispherical oscillatory coupling has never been specifically addressed.

In the present study we deliver single pulse TMS to M1 and calculated EEG–EEG coherence and power changes in the most prominent alpha- and beta band. We use this transient state of enhanced physiological oscillatory activity after TMS pulse and correlate it with the measurements of white matter structural integrity as expressed by diffusion tensor imaging. Whereas the scalp EEG is dominated by superficial cortical signals DTI can add information on connected deeper brain regions with an excellent resolution, i.e. microstructural integrity information of the networks involved. Thus this combination of approaches enables us to characterise the influence of deeper structures, e.g. thalamocortical, pathways on cortical oscillatory coupling.

Material and methods

Subjects

We studied 13 healthy subjects without any history of neurologic or psychiatric disorders (age 26.0 ± 2.4 years, 8 females). All patients underwent a detailed neurological assessment before recruitment. All subjects gave their written informed consent. The study was approved by the Ethical Committee of the Medical Faculty of the University of Kiel.

During the TMS-experiment, participants were seated in a reclining chair. Participants were asked to relax and close their eyes. The subjects wore earplugs with a white noise played at 80 dB to mask the TMS pulses.

Transcranial magnetic stimulation

TMS targeted the left M1 and the evoked motor response was recorded with surface EMG from contralateral first dorsal interosseous (FDI) muscle (Fig. 1). TMS was always given over the EEG cap. Single magnetic pulses were applied through a figure-of-eight coil (MC-B70) charged by a MagPro stimulator (MagVenture, Farum, Denmark). The pulses had a monophasic waveform and elicited a maximum current in the tissue in the posterior-anterior direction. We determined the site at which TMS evoked a maximal MEP in the right contralateral FDI muscle with the handle of the figure-of-eight coil pointing 45° posteriolaterally relative to the mid-sagittal line, and use this site for neuronavigation. The motor threshold of the relaxed right FDI was determined by assessing the stimulus intensity required to evoke an MEP of 50 mV in at least five out of ten trials [10,33]. For MEP measurements, the stimulation intensity was adjusted to evoke MEPs of approximately 0.75 mV at baseline. This stimulus intensity (SI 0.75 mV) was used to elicit MEPs throughout the experimental sessions. The reason for choosing MEPs of 0.75 mV instead of higher amplitudes was motivated by methodological considerations as we wished to induce focal M1 stimulation. Increasing the stimulation intensity the pulse might have involved more cortical regions or M1 inputs i.e. from pre-motor or associative cortical areas, leading to a more complex network interaction [11]. Moreover higher stimulation intensities would have increased the TMS artefact in the EEG recording. The mean stimulation intensity was 70.5 (±8.5 SD) of maximum stimulator output. The pulses were delivered every 5 s with a time jitter of 20%. We opted for a jitter in accordance with similar TMS/EEG studies [9] in order to reduce the influence of the TMS artefact for the further time and frequency domain analysis. Furthermore in similar TMS-EEG studies artefact clean data was analysed to achieve reliable spectral estimates [28,38]. We also wanted to minimize the influence of subject's anticipation of the timing of TMS on the recorded EEG activity. One hundred pulses were recorded.

Frameless stereotaxy (TMS-Navigator, Localite, Sankt Augustin, Germany) was used to navigate the TMS coil, to maintain and retain its exact location and orientation during the experimental session. Neuronavigation was based on coregistered individual T1-weighted magnetic resonance images of the whole brain (details see below).

EEG acquisition

The EEG was continuously recorded during TMS stimulation (10–20 system). To investigate the changes in the intra- and interhemispheric connectivity we distinctly selected the central motor/pre-motor area around the C3 electrode and recorded channel pairs close to stimulation site C3-F3 and C3-F7 [15]. On the other hand to investigate the interhemispheric coherence changes we recorded electrode pairs C3-C4 and CP5-CP6 but also P3-P4 as a site distal site for excluding possible confounds. EEG was recorded against a reference electrode located between Fz and Cz. Moreover two more electrodes were applied to both mastoids. Sintered Ag/AgCl ring electrodes with built-in 5 kΩ resistors were attached as a part of "EasyCap" (Falk-Minow Services, Herrsching-Breitbrunn, Germany). An MR-compatible EEG recording system "BrainAmp-MR" (Brain Products Co., Munich, Germany) was used to reduce the stimulation artefact. Electrode impedance was kept below 10 kΩ. One additional electrode was placed on the infraorbital ridge of the left eye for recording the vertical EOG and one was placed on the left perivertebral part of the lower back for acquisition of the electrocardiogram (ECG) to control for heartbeat artefacts. The data was transmitted via an optic fibre cable from the high-input impedance amplifier (250 Hz low-pass filter, 10 s time constant, 16-bit resolution, dynamic range 16.38 mV) to a personal computer. The TMS pulses were synchronized with the EEG amplifier (5-kHz sampling rate). Further studies might use higher sampling rates in order to better characterise the TMS artefact.

EEG data analysis

The EEG response of the single pulse TMS stimulation was analysed after the off-line visual inspection of the data. Artefact free segments were used for the analysis. Due to the continuous EEG acquisition the raw EEG signal included a TMS artefact induced by the magnetic pulse (about 5-ms duration with a rebound residual after ca 10–15 ms, Fig. 1). Artifacts were removed by cutting out 30-ms segments (from 5 ms prior to TMS onset to 25 ms after TMS pulse) from EEG for all TMS trials and electrodes. EEG data points before and after each removed segment were concatenated [9]. We used the non-cephalic reference as the sum of the signals between both mastoids to estimate large scale coherencies [4,8]. We applied this reference since it is well suitable to estimate coherences at intermediate and longer distances that might reveal additional correspondence with structural connectivity parameters [27]. We refrain from calculating the laplacian

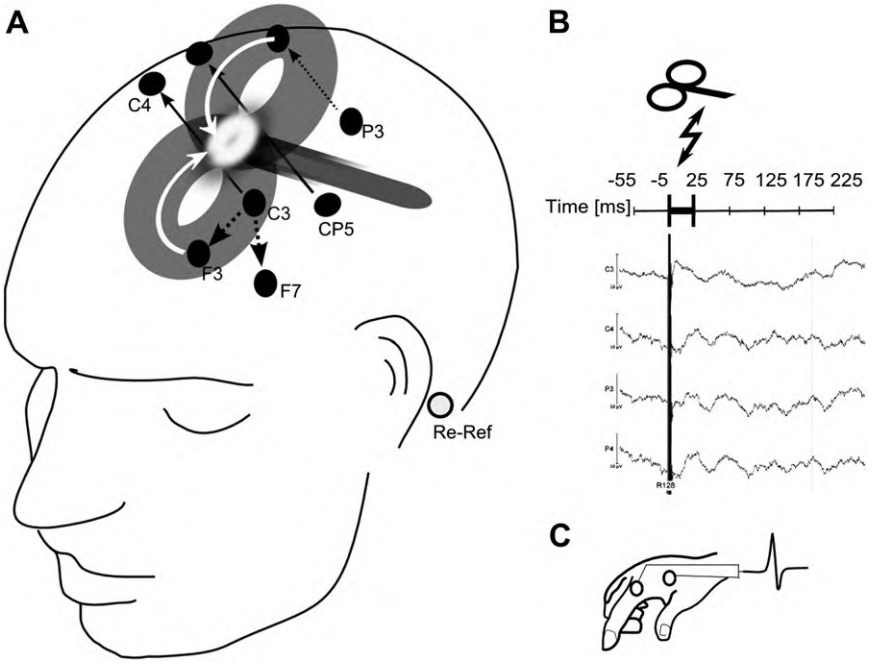

Figure 1. Experimental setup. (A) Schematic position and size of the magnetic coil. The direction of the current in the coil is showed in white lines. The EEG electrodes are presented as black circles. (B) EEG signal after the TMS pulse, together with the artefact and the analysed epochs are presented. (C) 100 muscle evoked potentials (MEP) were collected from the right first dorsal interosseus (FDI).

coherence since a big disadvantage of this method is that artefacts or noise within the recorded signal from other electrodes (for example at TMS stimulation site) significantly affect the calculated signal at multiple neighbouring sites [26]. Given the experimental setting of cortical coherence measurements with an expected physiological activity change by the TMS pulse we are aware that the traditional recordings might be erroneous rendered due to the lack of a quiet reference but the statistical basis of coherence data should be equivalent [12].

Coherence and power were estimated for epochs of 50 ms from −55 to −5 ms, 25 to 75 ms, 75 to 125 ms, and 125 to 175 ms to TMS pulse. Changes of coherence and power were then calculated as a quotient to baseline (−55 ms to −5 ms prior to TMS pulse, further as baseline) and epochs after TMS pulse. In order to examine whether the changes last longer the same statistical analysis was applied for epochs of 500 ms from −505 ms to −5 ms (as baseline_2) prior to TMS pulse and 25 ms to 525 ms after it.

Time frequency analysis

In this study the spectrum is estimated by multiplying the data with K different windows (i.e. tapers). The method uses a sliding time window for calculating the power spectrum by discrete Fourier transformation. If $x(t)$ is the signal, then the spectral power is calculated as follows [22,23]:

$$S_{\mathrm{MT}}(f) = \frac{1}{K}\sum_{k=1}^{K}\left|\tilde{X}_k(f)\right|^2 \tag{1}$$

$\tilde{X}_k(f)$ is the Fourier transform of the windowed signal $x(t)$ which can is calculated as

$$\tilde{X}_k(f) = \sum_{t=1}^{N} w_k(t)x(t)\exp(-2\pi ift), \tag{2}$$

and the terms $w_k(t)(K = 1, 2\ldots, K)$ are the K orthogonal tapers. In this study, $K = 7$ tapers were used. As orthogonal tapers with good leakage and spectral properties, the discrete prolate spheroidal sequences (DPSS) are applied [35]. The full description of the DPSS is given elsewhere [24].

After calculating the power spectra, the coherence between the two signals from the subjects, in our case between two cortical EEG signals $x(t)$ and $y(t)$, is estimated as follows [16]:

$$\hat{C}(f) = \frac{\left|\hat{S}_{xy}(f)\right|^2}{\hat{S}_{xx}(f)\hat{S}_{yy}(f)} \tag{3}$$

Here $S_{xy}(f)$ is the cross spectrum of both the individual power spectra $S_{xx}(f), S_{yy}(f)$ estimated as given in the above Equations (1) and (2), the overcap indicating the estimation [14].

The coherence is a linear measure between 0 and 1. When the estimated value for the coherence at a frequency is 0, this indicates the lack of correlation between the two signals at this frequency. The value 1 indicates complete correlation between the two signals at this frequency (Fig. 2). In this study, we used windows of 1000 ms length and the time step was 50 ms with the overlapping windows. So, each 50 ms overlapping window take into account the past 950 ms, totalling a window size of 1000 ms. Following the frequency resolution was 1 Hz (Fig. 2).

Statistical analyses

To test for TMS induced changes in cortico-cortical coherence we performed for the alpha (8–12 Hz) and beta range (13–30 Hz) coherence data one way ANOVA analyses with the within-subject factor *EEG channels* (C3-F3, C3-F7, C3-C4, CP5-CP6 P3-P4). If the ANOVA revealed a significant main effect the nature of these effect were explored with Fisher's LSD post-hoc pair-wise comparisons ($P < 0.05$; two-tailed). If the ANOVA was significant for the main effect we calculated a temporal sequence analyses for these channel pairs. To test for the duration of the studied effects we performed separate one way ANOVA analyses with the within-subject factor time *epochs* (4 levels, 25–75; 75–125; 125–175; 175–225 ms). The same statistical procedure was applied to EEG power data.

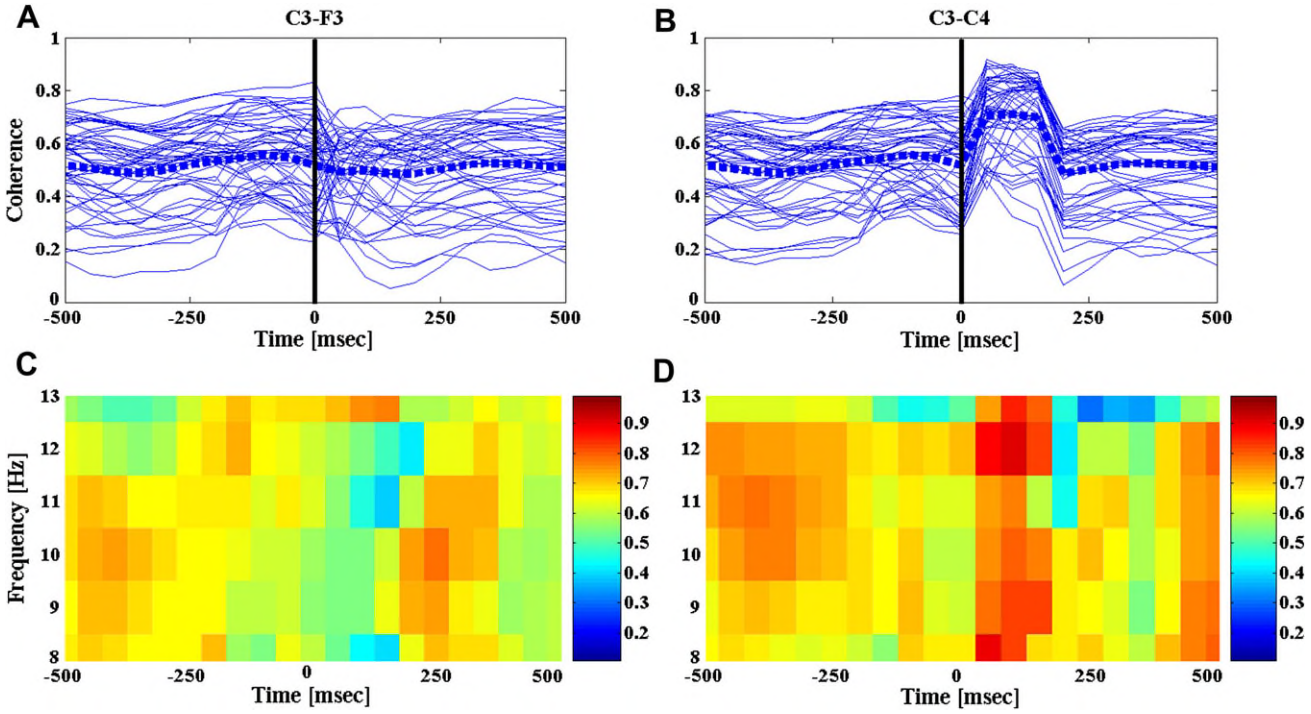

Figure 2. Analyses of cortico-cortical coherence after the TMS pulse. The single pulse coherences are plotted for an example subject for the electrode combination. (Plot A and C): no evident change in the coherence between ipsilateral electrode C3 and frontal electrode F3 for all the pulses before and after the TMS pulse at "0"ms in time marked with a solid line and the average of all the pulses are plotted as a dashed line. (Plot B and D): Alpha coherence is increased in the interhemispheric studied EEG electrodes C3-C4 and constant in the analysed intrahemispheric electrode pairs as shown for C3-F3.

In order to test if the MEP size predicts coherence changes we carried out a correlation analysis of this parameter to the coherence change for the studied electrode pairs.

Since we expected effects at the group level we refrain from building subgroups in dependence of gender or sex hormone levels during the menstrual cycle that might play a role for excitability changes in the intra- or interhemispheric functional connectivity [45].

Diffusion tensor imaging

We acquired diffusion-weighted (three acquisitions of 32 directions, b value 1000 s/mm, 5 b_0 images for each repetition, $2 \times 2 \times 2$ mm^3 voxels, 60 slices) and T1-weighted data at a 3 T Philips Achieva MR scanner. DTI data was acquired using a SENSE-Head-8 coil at a TE of 59 ms, TR 11,855 ms, matrix size 112×112, field of view $224 \times 224 \times 120$ mm, fat saturation on.

For neuronavigation T1 images were acquired. We used a standard MPRAGE sequence with an isotropic voxel resolution of 1 mm and sagittal slice orientation (TR 7.7 ms, TE 3.6 ms, flip angle 8°, 160 slices).

TBSS and DTI data analysis

The data was transformed to nifti format (dcm2nii, http://www.sph.sc.edu) and introduced into the further analysis using FMRIB Software Library (FSL, http://www.fmrib.ox.ac.uk/fsl/) and Tract-Based Spatial Statistics (TBSS). The detailed protocol is explained elsewhere [36]. In the following we only give a short description of the aspects relevant for the study. FA volumes form all subjects were nonlinearly aligned into a common space (MNI1521 mm) by the means of spline-based free-form deformation using the nonlinear registration tool (implemented in the FSL). A mean FA volume of all subjects was generated of all tracts common to the participants. The skeleton was thresholded at FA < 0.2. Using maximum FA values form the centres of the main tracts minimizes the confounding effects on the white-grey mark borders and tissue types. The skeletonised data was fitted into voxel-wise cross subject statistics.

For statistical analyses the randomize tool from the FSL package 4.1 (v 2.1) was used to carry out the permutation based cluster size statistics [25]. Clusters were defined by thresholding the raw t-statistics map of the skeleton at $t > 3$. The null distribution of the cluster size statistic was built up over 5000 random permutations of the effect of interest for the group statistics. The clusters were thresholded at $P < 0.05$, family-wise error rate (FWE) corrected for multiple comparisons. The age of the subjects and the rest motor threshold as studied by TMS were used as covariates of no interest to control for possible confounds, in the permutation based analyses of the interhemispheric coherence changes at C3-C4 and CP5-CP6 for the time interval (25–75 vs. baseline). Mean FA was calculated for the statistically significant cluster and plotted against the change of the effect of interest (Fig. 6).

Probabilistic diffusion tractography

To allow bias-free definition of seed and target areas unaffected by subjective judgements about anatomical correspondences, we used as suggested previously [1,2] all voxels in the significant region of the TBSS analysis as seeds. Moreover ROIs of left and right M1 areas have been built from the MNI probability atlas by including the entire area Broadman 4a with an exclusion of the medial cortical region at $x \pm 20$. We applied the probability distribution function (PDF) on fibre direction at each voxel of the diffusion data [2]. A multifiber model was fit to the diffusion data at each voxel, allowing for tracing of fibres through regions of crossing or complexity [1,2]. Here, we drew 5.000 streamline samples from our seeded voxels through these PDFs to form an estimate of the probability distribution of connections from each seeded voxel. When these streamlines reach a voxel in which more than one direction is estimated, they follow the direction that is closest and parallel with the direction at which the streamline arrives. Tracts

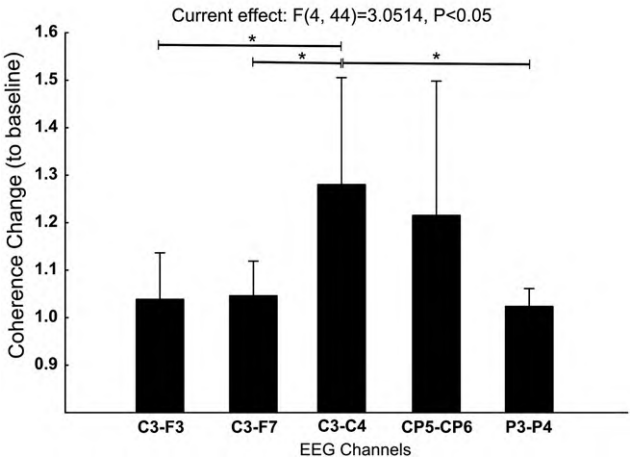

Figure 3. Coherence change for the analysed EEG electrodes for the first epoch in the analysed alpha band (quotient = coherence at 25–75 ms/coherence at −55 to −5 ms). Error bars represent standard deviation (SD). Asterisks (*) indicate significant contrasts.

generated by PDF are volumes wherein values at each voxel represent the number of samples (or streamlines) that passed through that voxel. For the elimination of spurious connections, tractography in individual subjects was thresholded to include only voxels through which at least 30 percent samples had passed [3]. These individual tracts were then binarized and summed across subjects and presented graphically (see Fig. 6). In these maps, each voxel value represents the number of subjects in whom the pathway passes through that voxel. To exclude regions with spurious connectivity, these probability maps were then thresholded to display only those paths that were present in a minimum of 30- and a maximum of 100 percent of subjects. For statistical analysis we extracted the FA values of skeleton data from the probabilistic tractography maps to include them into a single correlation analysis for the coherence changes in the main analysed electrode pair (C3-C4) for the first interval (25–75 ms to baseline).

Results

None of the participants reported adverse effects during or after the TMS session, EEG recordings or MRI scans.

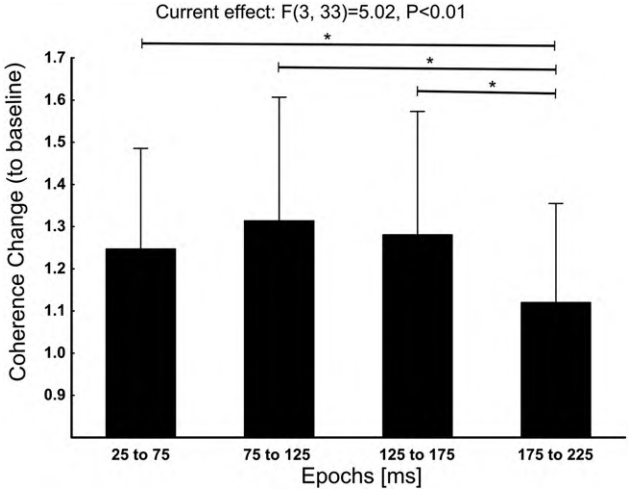

Figure 4. Temporal sequence of the coherence change in the alpha band for the C3-C4 electrode pairs after TMS pulse. Error bars represent standard deviation (SD). Asterisks (*) indicate significant contrasts.

Alpha coherence

The ANOVA model including the coherence change data for the first epoch (25–75 ms) was significant for the main effect *EEG channels* for the alpha coherence [$F(4, 48) = 2.89$, $P < 0.05$]. Post-hoc comparisons showed a higher coherence change in the channels C3-C4 in comparison to intrahemispheric C3-F3 ($P < 0.05$), C3-F7 ($P < 0.05$) or distal interhemispheric P3-P4 ($P < 0.01$) and no differences in comparison to the pair CP5-CP6. And indeed the coherence increased at C3-C4 (from 0.28 ± 0.16 to 0.33 ± 0.17) and CP5-CP6 (0.25 ± 0.16 to 0.28 ± 0.17), while in C3-F3, C3-F7, P3-P4 pairs no changes occurred (0.63 ± 0.18 to 0.63 ± 0.20, 0.75 ± 0.21 to 0.77 ± 0.20 and 0.85 ± 0.11 to 0.86 ± 0.08, Fig. 3). The coherence increase at CP5-CP6 in the first epoch was as well significant in comparison to P3-P4 ($P < 0.05$), and showed statistical trends in comparison to C3-F3 and C3-F7 ($P < 0.1$). The ANOVA for the second epoch (75–125 ms) was significant for the main effect *EEG channels* [$F(4, 48) = 3.63$, $P < 0.05$]. Similarly to the first epoch the post-hoc comparisons showed higher coherence changes in the channels C3-C4 in comparison to C3-F3 ($P < 0.005$), C3-F7 ($P < 0.005$) or interhemispheric P3-P4 ($P < 0.005$) and no changes in comparison to CP5-CP6. The other post-hoc tests were not significant. The ANOVAs for the third (125–175 ms) epoch showed a trend for the main effect *EEG channels* [$F(4, 48) = 2.40$, $P < 0.1$] and was not significant [$F(4, 48) = 0.92$, $P > 0.1$] for the fourth epoch (175–225 ms).

The analysis for the long lasting changes of the coherence (500 ms prior or $baseline_2$ and 500 ms after) was not significant for the main factor *EEG channels* [$F(4, 48) = 0.73$, $P > 0.1$]. The descriptive statistics of this interval reveals however relative coherence changes in the interhemispheric channel pairs (C3-C4 and CP5-CP6, an increase from 0.25 ± 0.09 to 0.27 ± 0.10 for C3-C4 and from 0.23 ± 0.16 to 0.25 ± 0.15 for the channel pair CP5-CP6 respectively).

The ANOVA for the duration of the coherence changes with the within-subject factor *epochs* was significant for the electrodes C3-C4 ([$F(3, 33) = 5.02$, $P = 0.006$], Fig. 4). The post-hoc tests revealed that the main effect was caused by significant differences in the last epoch (175–225 ms) in comparison to first three ($P < 0.05$ at 25–75 ms; $P < 0.01$ at 75–125 ms and $P < 0.01$ for the 125–175 ms interval, respectively). The ANOVA for the channel pair CP5-CP6 was not significant for the main effect *epochs*.

Beta coherence

The ANOVA model for the coherence change in the beta frequency range was not significant for the main effect *EEG channels* [$F(4, 48) = 1.17$, $P > 0.1$] for the first epoch (25–75 ms). The analysis for the long lasting changes of the coherence in the beta band (500 ms prior and 500 ms after the TMS pulses) was not significant for the main factor *EEG channels* [$F(4, 48) = 0{,}06$, $P > 0.1$].

Alpha power

The ANOVA calculated for power changes in the first epoch (25–75 ms) was not significant for the main effect *EEG channels* [$F(7, 49) = 0.82$, $P > 0.1$]. The analysis for the long lasting changes (500 ms prior and 500 ms after the TMS pulses) was not significant for the main effect [$F(7, 84) = 1.12$, $P > 0.1$].

Beta power

The ANOVA calculated for power changes in the beta band was not significant for the main effect *EEG channels* [$F(7, 49) = 1.03$, $P > 0.1$] for the first epoch (25–75 ms). The analysis for the long lasting changes of power (500 ms prior and 500 ms after the TMS pulses, Fig. 5) was significant for the main factor *EEG channels*:

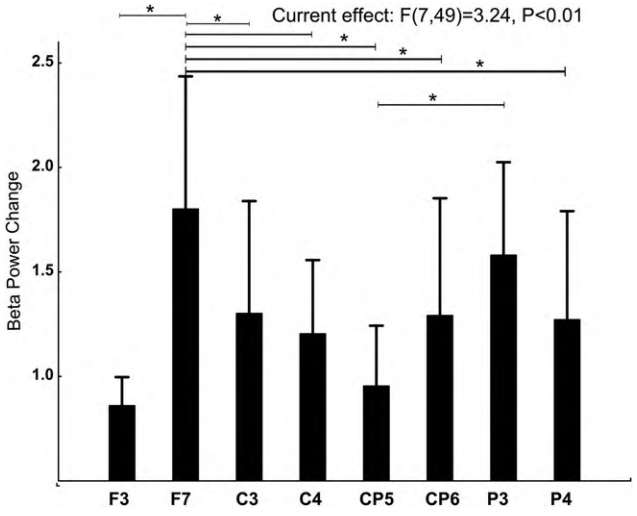

Figure 5. Power changes in the beta band for the analysed EEG electrodes for 500 ms epochs (quotient = coherence at 25–525 ms/coherence at −505 to −5 ms). Error bars represent standard deviation (SD).

[$F(7, 49) = 3.24$, $P < 0.01$]. The post-hoc tests revealed that the main effect was caused by significant differences between beta power changes at channels F3 (0.86 ± 0.1) vs. F7 (1.80 ± 0.63, $P < 0.001$) and F3 vs. P3 (1.58 ± 0.44, $P < 0.001$), but also F7 vs. C3 (1.30 ± 0.54, $P < 0.05$), F7 vs. C4 (1.20 ± 0.35, $P < 0.01$), F7 vs. CP5 (0.95 ± 0.29, $P < 0.005$), F7 vs. CP6 (1.29 ± 0.56, $P < 0.05$) and F7 vs. P4 (1.27 ± 0.52, $P < 0.05$). Moreover the comparison CP5 vs. P3 was also significant ($P < 0.01$).

Correlation MEP and coherence

The correlation analyses of MEP amplitude and coherence changes in interhemispheric but also in intrahemispheric channel pairs were not significant nor showed any statistical trends for alpha and beta band ($P > 0.1$).

Imaging data

Conventional MRI T1 images revealed no structural abnormalities and presented no macroscopic differences in the studied subjects.

To test the relationship between functional connectivity as indicated by the changes in coherence and structural connectivity represented by white matter microstructure across subjects, we used TBSS, permutation analysis and FA estimates. To analyse the cortical and subcortical correlates of the coherence change our analysis was not restricted to a region of interest but included the entire brain. For the main studied effects (coherence change at C3-C4 at 25–75 in comparison to baseline and coherence change at CP5-CP6), the TMS induced functional connectivity change positively correlated with FA in white matter tracts in the proximity of the contralateral thalamus or the perithalamic white matter (center of gravity $(COG)_{(x,y,z)}$ at 24, −29, 0; $t > 3$, $P < 0.05$ FWE corrected for multiple comparisons, cluster size: 146 voxels; Fig. 6) and in adjacent areas for the channel pair CP5-CP6 ($COG_{(x,y,z)}$ at 20, −23, −3; $t > 3$, $P < 0.05$, FWE cluster corrected for multiple comparisons, cluster size: 155 voxels; Fig. 6).

The correlation analysis of FA values extracted from the tract between bilateral M1 areas and coherence change in the first interval (25–75 ms to baseline) at the electrodes C3-C4 was significant ($r = 0.56$; $P < 0.05$, Fig. 6). The correlation analysis of FA from the tract between the contralateral thalamus and M1 and coherence change (C3-C4, 25–75 ms to baseline) showed a positive statistical trend ($r = 0.48$; $P < 0.1$, Fig. 7).

Discussion

In this study we demonstrate that suprathreshold TMS of the primary motor cortex induces changes in the coupled cortical oscillatory activity. TMS pulses generate an increase in the interhemispheric coherence in the alpha band in the stimulated central regions and did not affect intra- and interhemispheric oscillatory coupling at distant sites studied. The induced changes did not last longer than 200 ms after the TMS pulse. There was no significant modulation of the beta band coherence. The power changes

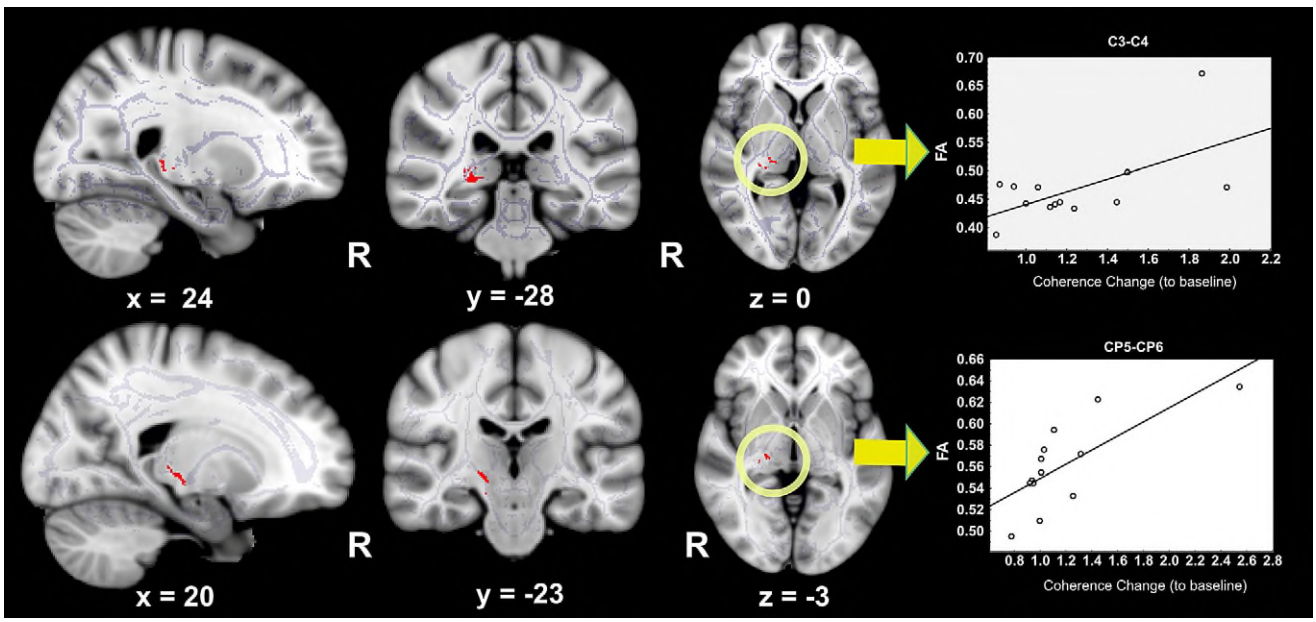

Figure 6. Whole brain analysis for correlation between FA and coherence change for the epoch 25–75 ms to baseline. Top line. Cluster showing a significant positive correlation for the electrodes C3-C4. Bottom line. Cluster showing a significant positive correlation for the electrodes CP5-CP6. Right panel: mean FA values from the significant cluster plotted against the coherence change.

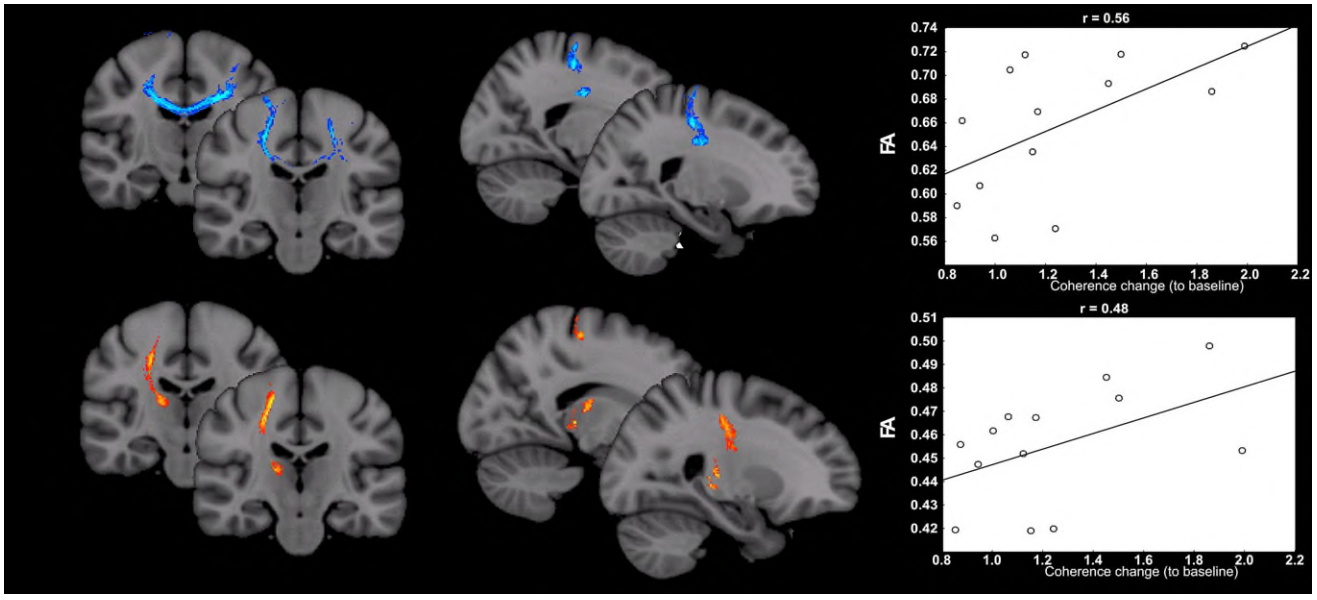

Figure 7. Probabilistic tractography results. Maps, showing voxel values represented by the number of subjects in whom the pathways passes through that voxel. Voxels with higher connectivity values are brighter. Top line in blue. Pathways between both M1 areas. Bottom line in red-yellow. Pathways between significant contralateral perithalamic cluster and M1 structures. Right panel: mean FA values extracted from the significant clusters and plotted against coherence change in the epoch 25–75 ms to baseline for the electrode pair C3-C4.

analysis revealed an unspecific increase in beta band over wide spread cortical areas as previously reported [29]. By the aid of DTI we could describe the microstructural correlate for the observed changes in coherence. Using regional FA as microstructure integrity marker, we found that the white matter in the vicinity of the contralateral thalamus as well as in transcallosal fibre tracts showed a linear relationship with the strength of TMS induced modulation of interhemispheric oscillatory alpha coupling.

The present study confirms that single pulse TMS modulates the physiological oscillatory activity not only at the stimulation site but also in interconnected cortical areas [34]. As the experiments were conducted at rest it is plausible that the alpha rhythm as the prominent idling rhythm of the human brain prevailing in the primary motor cortex was mainly modified. This is in keeping with previous studies which found that alpha rhythm was significantly affected by single pulse TMS of M1 in a similar setting [9]. Moreover these results support the hypothesis that single pulse TMS does not produce new artificial oscillatory activity but rather entrains and enhances the physiological oscillations [32,41].

To investigate the involved interconnected cortical areas reflecting the network effects of the TMS we analysed cortico-cortical coherence. In the alpha band we observed only a slight, non significant increase of the coherence between left-hemispheric pre-motor and frontal electrode pairs (C3-F3, C3-F7), while the main modulation occurred in interhemispheric electrodes underlying the homologous stimulated area. There was a significant increase of alpha band coherence in both central EEG channel pairs C3-C4 and CP5-CP6. The evoked changes were topographically specific since no coherence change was detected in the distant interhemispheric electrode pairs P3-P4. This effect on interhemispheric coupling confirms previous TMS-EEG studies and is likely related to the modulation of the interconnected contralateral corresponding areas by motor cortex TMS [9,31]. Transcallosal pathways linking homologous cortical areas in both hemispheres are likely to play a role in this [7,39,43]. This is supported in our study by the positive linear relationship between regional FA values in the relevant part of the corpus callosum and the TMS induced change in interhemispheric alpha-coherence. This is in line with a recent study that applied probabilistic tractography and simultaneous TMS-EEG recordings and revealed a significant relationship between microstructural integrity of callosal motor fibres and TMS induced interhemispheric signal propagation from left to right motor cortex [43]. A recent study showed a correlation of the interhemispheric inhibition as studied by paired pulse TMS and fractional anisotropy from DTI [44].

Interestingly, it was the microstructure in the proximity of the contralateral to the stimulation site thalamus that presented the main significant correlation with the alpha band coherence change between the two hemispheres. The thalamus plays an important role for cortical oscillatory activity [37]. The intrinsic micro-architecture might enable thalamus to act as pacemaker of oscillations at different frequencies including alpha oscillations [37]. A pathological alpha rhythm was found over the affected hemisphere in patients with unilateral subcortical ischaemia [30]. Moreover Parkinson's disease patients after thalamotomy express abnormally less beta oscillations after the TMS pulse, possibly due to the involvement of cortico-thalamic feedback loops [42]. These connections maintain and enhance such oscillations. However, in contrast to ipsilateral thalamocortical projections, there are only weak thalamic projections to the contralateral hemisphere, thus the thalami alone are unlikely to be responsible for the trans-hemispheric linkage observed in the present study. Rather the transcallosal pathway described on the basis of probabilistic tractography might represent the primary anatomical basis for the coupling between the areas, whereas the contralateral thalamus and thalamocortical pathway might modulate or maintain the oscillatory nature of the observed changes in coupling between the pericentral regions in response to TMS.

Given all the evidence from TMS-EEG studies we can assume that the oscillatory activity is enhanced in the modules to which the TMS pulse is applied but a complementary synchronisation of the contralateral hemisphere might evolve [32]. It has been previously shown that excitatory stimuli, e.g. the TMS pulse to the ipsilateral motor cortex, can enhance cortical oscillations without an 'active' change in thalamic excitability but the constant 'tonic' drive through the thalamocortical loops seems to be crucial to modulate

this rhythmic cortical activity [5]. Equally, under inhibitory influences to the cortex the thalamocortical drive has to be increased to maintain oscillatory cortical activity [5]. Single pulse TMS to M1 have mainly an inhibitory influence on the contralateral M1 and this might be related to the described changes of alpha activity [20]. Thus it is plausible that the coupled oscillatory alpha activity in the contralateral cortex is more dependent on a strong thalamocortical projection than in the ipsilateral hemisphere, where the TMS pulse induces a motor cortical excitation and synchronisation. Since the coherence data is calculated as a quotient to the prestimulus activity we show that coupled alpha oscillations present a state dependency that is presumably modified by the cortico-thalamic network. Whether a change of the ground frequency to alpha band from other frequencies occurred after TMS pulses and which is the importance of the subcortical structures for the ground rhythm modulation might be interesting questions for further studies using a similar approach.

The power changes presented in our study confirm previous work [9,29]. Changes in beta band were noted in different episodes of preparation and execution of a motor program [18,21]. The distinct long lasting beta power changes in the electrodes close to the stimulation site F3 and F7 could deflect an "activation" (EEG power decrease) of these areas by the TMS pulse. We refrained to use power changes as marker of functional connectivity because of the lack of topographic and event specificity.

In conclusion we confirm that single pulse TMS transiently enhances cortical alpha oscillations and interhemispheric oscillatory coupling, while beta band remained unchanged under the studied conditions. Using TMS-EEG and DTI-imaging we can show that not only the transcallosal pathway but also the thalamocortical fibres especially in the contralateral hemisphere modulate the coupled oscillations. This is in keeping with previous hypotheses on transcallosal effects of single pulse TMS and the role of thalamocortical loops in oscillatory cortical activity. The combination of EEG and advanced MRI-imaging techniques is a powerful approach to examine physiological brain networks after TMS-enhancement.

References

[1] Behrens TEJ, Berg HJ, Jbabdi S, Rushworth MFS, Woolrich MW. Probabilistic diffusion tractography with multiple fibre orientations: what can we gain? Neuroimage 2007;34:144–55.

[2] Behrens TEJ, Woolrich MW, Jenkinson M, Johansen-Berg H, Nunes RG, Clare S, et al. Characterization and propagation of uncertainty in diffusion-weighted MR imaging. Magn Reson Med 2003;50:1077–88.

[3] Boorman ED, O'Shea J, Sebastian C, Rushworth MFS, Johansen-Berg H. Individual differences in white-matter microstructure reflect variation in functional connectivity during choice. Curr Biol 2007;17:1426–31.

[4] Chen ACN, Rappelsberger P. Brain and human pain: topographic EEG amplitude and coherence mapping. Brain Topogr 1994;7:129–40.

[5] Destexhe A, Contreras D, Steriade M. Cortically-induced coherence of a thalamic-generated oscillation. Neuroscience 1999;92:427–43.

[6] Di Lazzaro V, Oliviero A, Pilato F, Saturno E, Dileone M, Meglio M, et al. Direct recording of the output of the motor cortex produced by transcranial magnetic stimulation in a patient with cerebral cortex atrophy. Clin Neurophysiol 2004; 115:112–5.

[7] Engel AK, Fries P, Singer W. Dynamic predictions: oscillations and synchrony in top-down processing. Nat Rev Neurosci 2001;2:704–16.

[8] Essl M, Rappelsberger P. EEG cohererence and reference signals: experimental results and mathematical explanations. Med Biol Eng Comput 1998;36:399–406.

[9] Fuggetta G, Fiaschi A, Manganotti P. Modulation of cortical oscillatory activities induced by varying single-pulse transcranial magnetic stimulation intensity over the left primary motor area: a combined EEG and TMS study. Neuroimage 2005;27:896–908.

[10] Groppa S, Oliviero A, Eisen A, Quartarone A, Cohen LG, Mall V, et al. A practical guide to diagnostic transcranial magnetic stimulation: Report of an IFCN committee. Clin Neurophysiol 2012;123:858–82.

[11] Groppa S, Schlaak BH, Munchau A, Werner-Petroll N, Dunnweber J, Baumer T, et al. The human dorsal premotor cortex facilitates the excitability of ipsilateral primary motor cortex via a short latency cortico-cortical route. Hum Brain Mapp 2012b;33:419–30.

[12] Guevara MA, Corsi-Cabrera M. EEG coherence or EEG correlation? Int J Psychophysiol 1996;23:145–53.

[13] Hallett M. Transcranial magnetic stimulation: a primer. Neuron 2007;55:187–99.

[14] Halliday DM, Rosenberg JR, Amjad AM, Breeze P, Conway BA, Farmer SF. A framework for the analysis of mixed time series/point process data–theory and application to the study of physiological tremor, single motor unit discharges and electromyograms. 1995. p. 237.

[15] Herwig U, Kolbel K, Wunderlich AP, Thielscher A, von Tiesenhausen C, Spitzer M, et al. Spatial congruence of neuronavigated transcranial magnetic stimulation and functional neuroimaging. Clin Neurophysiol 2002;113: 462–8.

[16] Jarvis MR, Mitra PP. Sampling properties of the spectrum and coherency of sequences of action potentials. MIT Press; 2001. pp. 717–749.

[17] Jones EG. The thalamic matrix and thalamocortical synchrony. Trends Neurosci 2001;24:595–601.

[18] Marsden J, Werhahn K, Ashby P, Rothwell J, Noachtar S, Brown P. Organization of cortical activities related to movement in humans. J Neurosci 2000;20: 2307.

[19] Massimini M, Ferrarelli F, Huber R, Esser SK, Singh H, Tononi G. Breakdown of cortical effective connectivity during sleep. Science 2005;309:2228–32.

[20] Meyer BU, Roricht S, Grafin von Einsiedel H, Kruggel F, Weindl A. Inhibitory and excitatory interhemispheric transfers between motor cortical areas in normal humans and patients with abnormalities of the corpus callosum. Brain 1995;118(Pt 2):429–40.

[21] Mima T, Matsuoka T, Hallett M. Functional coupling of human right and left cortical motor areas demonstrated with partial coherence analysis. Neurosci Lett 2000;287:93–6.

[22] Mitra PP, Pesaran B. Analysis of dynamic brain imaging data. Biophys J 1999a; 76:691–708.

[23] Mitra PP, Pesaran B. Analysis of dynamic brain imaging data. Elsevier; 1999b. pp. 691–708.

[24] Muthuraman M, Galka A, Deuschl G, Heute U, Raethjen J. Dynamical correlation of non-stationary signals in time domain–a comparative study. Biomed Signal Processing Control 2010;5:205–13.

[25] Nichols TE, Holmes AP. Nonparametric permutation tests for functional neuroimaging: a primer with examples. Hum. Brain Mapp 2002;15:1–25.

[26] Niedermeyer E, Da Silva FHL. Electroencephalography: basic principles, clinical applications, and related fields. Lippincott Williams & Wilkins; 2005.

[27] Nunez PL, Srinivasan R, Westdorp AF, Wijesinghe RS, Tucker DM, Silberstein RB, et al. EEG coherency: I: statistics, reference electrode, volume conduction, Laplacians, cortical imaging, and interpretation at multiple scales. Electroencephalogr Clin Neurophysiol 1997;103:499–515.

[28] Oliviero A, Strens LHA, Di Lazzaro V, Tonali PA, Brown P. Persistent effects of high frequency repetitive TMS on the coupling between motor areas in the human. Exp Brain Res 2003;149:107–13.

[29] Paus T, Sipila PK, Strafella AP. Synchronization of neuronal activity in the human primary motor cortex by transcranial magnetic stimulation: an EEG study. J Neurophysiol 2001;86:1983–90.

[30] Pfurtscheller G, Sager W, Wege W. Correlations between CT scan and sensorimotor EEG rhythms in patients with cerebrovascular disorders. Electroencephalogr Clin Neurophysiol 1981;52:473–85.

[31] Rizzo V, Siebner HS, Morgante F, Mastroeni C, Girlanda P, Quartarone A. Paired associative stimulation of left and right human motor cortex shapes interhemispheric motor inhibition based on a Hebbian mechanism. Cereb Cortex 2009;19:907–15.

[32] Rosanova M, Casali A, Bellina V, Resta F, Mariotti M, Massimini M. Natural frequencies of human corticothalamic circuits. J Neurosci 2009;29: 7679–85.

[33] Rossini PM, Barker AT, Berardelli A, Caramia MD, Caruso G, Cracco RQ, et al. Non-invasive electrical and magnetic stimulation of the brain, spinal cord and roots: basic principles and procedures for routine clinical application. Report of an IFCN committee. Electroencephalogr Clin Neurophysiol 1994; 91:79–92.

[34] Siebner H, Peller M, Bartenstein P, Willoch F, Rossmeier C, Schwaiger M, et al. Activation of frontal premotor areas during suprathreshold transcranial magnetic stimulation of the left primary sensorimotor cortex: a glucose metabolic PET study. Hum Brain Mapp 2001;12:157–67.

[35] Slepian D. Prolate spheroidal wave functions, Fourier analysis, and uncertainty. V-The Discrete Case; 1978:1371–430.

[36] Smith SM, Jenkinson M, Johansen-Berg H, Rueckert D, Nichols TE, Mackay CE, et al. Tract-based spatial statistics: voxelwise analysis of multi-subject diffusion data. Neuroimage 2006;31:1487–505.

[37] Steriade M, Amzica F. Intracortical and corticothalamic coherency of fast spontaneous oscillations. Proc Natl Acad Sci USA 1996;93:2533–8.

[38] Strens LH, Fogelson N, Shanahan P, Rothwell JC, Brown P. The ipsilateral human motor cortex can functionally compensate for acute contralateral motor cortex dysfunction. Curr Biol 2003;13:1201–5.

[39] Terada K, Usui N, Umeoka S, Baba K, Mihara T, Matsuda K, Tottori T, Agari T, Nakamura F, Inoue Y. Interhemispheric connection of motor areas in humans. J Clin Neurophysiol 2008;25:351–6.

[40] Thut G, Miniussi C. New insights into rhythmic brain activity from TMS-EEG studies. Trends Cogn Sci 2009;13:182–9.

[41] Thut G, Veniero D, Romei V, Miniussi C, Schyns P, Gross J. Rhythmic TMS causes local entrainment of natural oscillatory signatures. Curr Biol 2011;21: 1176–85.

[42] Van Der Werf YD, Sadikot AF, Strafella AP, Paus T. The neural response to transcranial magnetic stimulation of the human motor cortex. II. Thalamocortical contributions. Exp Brain Res 2006;175:246–55.
[43] Voineskos AN, Farzan F, Barr MS, Lobaugh NJ, Mulsant BH, Chen R, et al. The role of the corpus callosum in transcranial magnetic stimulation induced interhemispheric signal propagation. Biol Psychiatry 2010;68:825–31.
[44] Wahl M, Lauterbach-Soon B, Hattingen E, Jung P, Singer O, Volz S, et al. Human motor corpus callosum: topography, somatotopy, and link between microstructure and function. J Neurosci 2007;27:12132–8.
[45] Weis S, Hausmann M, Stoffers B, Sturm W. Dynamic changes in functional cerebral connectivity of spatial cognition during the menstrual cycle. Hum Brain Mapp 2011;32:1544–56.